arXiv:1303.4587v1 [hep-ph] 19 Mar 2013

Constraints on electromagnetic properties of sterile neutrinos from MiniBooNE results

A. A. Radionov*[1,2]

[1]Institute for Nuclear Research of the Russian Academy of Sciences,
60th October Anniversary Prospect, 7a, 117312 Moscow, Russia
[2]Faculty of Physics, Moscow State University, Vorobjevy Gory, 119991 Moscow, Russia

March 20, 2013

Abstract

In the class of models with small mixing between sterile and active neutrinos we place constraints on effective muon-to-sterile neutrino transition magnetic and electric dipole moments from the combined MiniBooNE results for the mass range of sterile neutrino 10 MeV $< m_s <$ 500 MeV. Our results are valid for models with CP-violating interactions, for the Dirac and the Majorana sterile neutrino. Also we show that such dipole electromagnetic interactions can not be the main source of the anomalous events in the MiniBooNE experiment, because they fail to reproduce the anomalous event distribution of polar angle (meanwhile, for some values of magnetic and electric moments there would be a good agreement with the anomalous event distribution of reconstructed energy).

1 Introduction

In last decades significant progress in experimental studies of neutrinos is achieved. Because of the incompleteness of Standard model of particle physics especially in this field, many questions about neutrino properties have been arisen. A Mini–Booster Neutrino Experiment (MiniBooNE) observes a so-called ”anomaly”: statistically significant excess of detected events at low energies in comparison with theoretical predictions [1, 2, 3]. Much efforts have been already spent and several hypotheses have been put forward to explain this phenomenon (see a list in e.g. [3]).

One of the hypothesis consists in introducing sterile neutrino of mass in the range 40-600 MeV, which is unstable with respect to radiative decay. There are two realizations of this idea in literature. First: sterile neutrinos are produced by flavor mixing with active (muon) neutrinos [4, 5] at scattering of latter off nuclei due to neutral current weak interactions ($\nu_\mu \to \nu_s$), and subsequently radiatively decay due to a transition moment ($\nu_s \to \nu\gamma$). This idea has been already tested experimentally with negative result [6]. Thus, only a region of mass 400-600 MeV [7] remains allowed and waits for a special analysis of data from c- and b-factories [8]. Second: it was argued [9] that the dipole transition moment may also be responsible for both sterile neutrino production

---

[*] radionov@ms2.inr.ac.ru

and decay. In this case, it is a dipole transition moment between sterile and muon neutrinos, which does the main job. Anyway, the suggested explanations have renewed interest to dipole transition moments of hypothetical heavy sterile neutrinos.

In this paper we extract new and improve old [10] limits on values of sterile-to-muon neutrino transition dipole moments under condition that we can neglect flavor mixing between sterile and active neutrinos. To this end we analyze the results of the MiniBooNE detector [11], which measures Charge-Current-like and Neutral-Current-like events from neutrino and antineutrino fluxes. These fluxes are mainly composed of muon neutrinos and antineutrinos with energies 200 MeV $< E_\nu <$ 3 GeV. The detector cannot distinguish photon events from electron/positron events [1], so neutrino transition dipole moments can be probed, because transition moments lead to a photoproduction in the detector.

The paper is organized as follows. Section 2 describes what are neutrino transition dipole moments and introduces useful parametrization of them; then we calculate a cross section of active-to-sterile (anti)neutrino conversion on an atom and sterile (anti)neutrino radiative decay rates. Section 3 contains a probability function of sterile neutrino decay inside the MiniBooNE detector and the distributions of the expected photons of energy and polar angle. In particular, we show here that neutrinos, produced on nuclei and atomic electrons via exchange of massless particles (photons), as well as the photons from their decay are mostly forward, so fail to reproduce the event excess as function of polar angle [1, 2]. Section 4 describes methods which we exploit to put constraints on dipole transition moments and summarizes our results and describes (possibly) relevant for the MiniBooNE anomaly extensions of the model.

2 Model description

Here we describe a model with the Dirac sterile neutrinos. The case of the Majorana neutrinos requires minor modifications, which are listed in the end of this Section.

The most general Lorenz-invariant dipole electromagnetic interaction between neutrinos and an electromagnetic field is:

$$\mathcal{L}_{int} = \frac{1}{2}\sum_{\substack{i,j=1\\ i\leq j}}^{N_\nu} \overline{\nu}_j \left(\mu_{ij} + \gamma_5 d_{ij}\right) \sigma_{\mu\nu} \mathcal{F}^{\mu\nu} \nu_i + \text{h.c.}\,, \tag{1}$$

where ν_i are neutrino fields in the mass basis, N_ν is a number of neutrinos, $\mu^{tr}_{ij} \equiv \mu_{ij}\left(d^{tr}_{ij} \equiv d_{ij}\right)$ with $i \neq j$ are magnetic (electric) transition dipole moments between massive neutrinos i and j, μ_{ii} (d_{ii}) are diagonal magnetic (electric) transition dipole moments, $\mathcal{F}^{\mu\nu} = \partial^\mu A^\nu - \partial^\nu A^\mu$ is an electromagnetic field strength tensor and $\sigma_{\mu\nu} = \frac{i}{2}\left(\gamma_\mu\gamma_\nu - \gamma_\nu\gamma_\mu\right)$, where γ_μ are the Dirac matrices. We investigate a model with $N_\nu = 4$, so we suppose an existence of one additional sterile neutrino[1] with a mass m_s.

For our study it is convenient to work with gauge (flavor) states in the *active neutrino sector*. Sterile neutrino ν_s is a massive fermion neutral with respect to the Standard model gauge group. We are interested in a situation where flavor mixing between sterile and active neutrino is negligible, so that sterile neutrino in flavor basis ν_s and the heaviest neutrino in mass basis ν_4 are almost the same: $\nu_4 \simeq \nu_s$. We denote the mass of sterile neutrino mass by m_s.

---

[1] We extend the analysis to models with $N_\nu > 4$ case in Section 4.

Interaction (1) would induce two processes: an active-sterile neutrino conversion on atomic electrons and nuclei and sterile neutrino decay back to active neutrino (and photon).

The transition dipole moments entering (1) are related to dipole moments in the flavor basis through relations:

$$\begin{array}{c} \mu_{\alpha\beta} = \sum_{i,j=1}^{4} \mu_{ij} U_{\alpha i}^{*} U_{\beta j} \ , \\ d_{\alpha\beta} = \sum_{i,j=1}^{4} d_{ij} U_{\alpha i}^{*} U_{\beta j} \ , \end{array} \tag{2}$$

where $U_{\alpha i}$ is a generalization of the Pontecorvo–Maki–Nakagawa–Sakata matrix:

$$\nu_{\alpha}(x) = \sum_{i} U_{\alpha i} \nu_{i}(x) \ . \tag{3}$$

It is convenient also to define them in another basis:

$$\begin{array}{c} \mu_{\alpha j} = \sum_{i=1}^{4} \mu_{ij} U_{\alpha i}^{*} \ , \\ d_{\alpha j} = \sum_{i=1}^{4} d_{ij} U_{\alpha i}^{*} \ . \end{array} \tag{4}$$

In this paper we are mostly interested in the following term:

$$\mathcal{L}_{int}' = \frac{1}{2} \overline{\nu}_4 \left(\mu_{\mu 4}^{tr} + \gamma_5 d_{\mu 4}^{tr} \right) \sigma_{\rho\lambda} \mathcal{F}^{\rho\lambda} \nu_{\mu} + \text{h.c.} \ . \tag{5}$$

The undertaken analysis described bellow allows us to place constraints on the quantity:

$$\kappa_{\mu 4}^{tr} \equiv \sqrt{|\mu_{\mu 4}^{tr}|^2 + |d_{\mu 4}^{tr}|^2} \ . \tag{6}$$

Generally, electric and magnetic moments are complex quantities which have different phases. We parametrize them in the form:

$$\mu_{\mu 4}^{tr} \equiv \kappa_{\mu 4}^{tr} \cos\left(\lambda_{\mu 4}^{tr}\right) \exp\left(i\phi_{\mu 4}^{tr}\right) \quad \text{and} \quad d_{\mu 4}^{tr} \equiv \kappa_{\mu 4}^{tr} \sin\left(\lambda_{\mu 4}^{tr}\right) \exp\left(i\chi_{\mu 4}^{tr}\right) \ , \tag{7}$$

where $\lambda_{\mu 4}^{tr}$, $\phi_{\mu 4}^{tr}$ and $\chi_{\mu 4}^{tr}$ are real-valued parameters. Analogous notations are adopted for transition moments in the mass basis:

$$\mu_{4i}^{tr} \equiv \kappa_{4i}^{tr} \cos\left(\lambda_{4i}^{tr}\right) \exp\left(i\phi_{4i}^{tr}\right) \quad \text{and} \quad d_{4i}^{tr} \equiv \kappa_{4i}^{tr} \sin\left(\lambda_{4i}^{tr}\right) \exp\left(i\chi_{4i}^{tr}\right) \ , \tag{8}$$

where λ_{4i}^{tr}, ϕ_{4i}^{tr} and χ_{4i}^{tr} are real-valued parameters.

In the MiniBooNE detector the conversion of muon (anti)neutrino to sterile (anti)neutrino would happen mostly on carbon atoms bounded in oil. In the quasi-elastic approximation the conversion cross section contains a form factor which depends on a single parameter $t = -q^2$ (where q is a 4-momentum transfer carried by photon), and was given in [12]. It was used in previous studies of sterile neutrino transition magnetic moments [9, 10] (in Ref. [9] a different nuclear part of the form factor was adopted for large $t > 10^{-3}$ GeV^2, however, the main contribution comes from atomic and coherent nuclear processes, where t is smaller, so the difference is insignificant). In the case of light nucleus (carbon: numbers of protons and neutrons are $Z = 6$ and $A = 12$ respectively) an analytical expression for the form factor is [12]:

$$G^2(t) = \begin{cases} \frac{Z^2 a^4 t^2}{(1+a^2 t)^2} + \frac{Z a'^4 t^2}{(1+a'^2 t)^2}, & t < t_0; \ \text{(atomic part of the form factor)} \ , \\ \frac{Z^2}{\left(1+\frac{t}{d}\right)^2}, & t > t_0; \ \text{(nuclear part of the form factor)} \ , \end{cases} \tag{9}$$

where $a = 184.15 \times (2.718)^{-1/2} Z^{-1/3}/m_e$, $a' = 1194 \times (2.718)^{-1/2} Z^{-2/3}/m_e$ and $d = 0.164 \times A^{-2/3}\text{GeV}^2$ [12]; $t_0 = 7.39 \times m_e^2$ [10] (m_e is electron mass).

For the differential cross section of muon neutrino conversion into sterile neutrino of positive $d\sigma_{+,\nu}$ and negative $d\sigma_{-,\nu}$ chirality, we obtain:

$$\frac{d\sigma_{\mp}^{\nu}(E,\theta,\phi)}{d\cos\theta d\phi} = \frac{\alpha\left(\kappa_{\mu4}^{tr}\right)^2}{4\pi}\left(1 - \sin\left(2\lambda_{\mu4}^{tr}\right)\cos\left(\phi_{\mu4}^{tr} - \chi_{\mu4}^{tr}\right)\right)\frac{G^2(t)}{t^2}vE^4(1\pm v)^3(1\mp\cos\theta) \ , \quad (10)$$

where $\kappa_{\mu4}^{tr}$, $\lambda_{\mu4}^{tr}$, $\phi_{\mu4}^{tr}$, $\chi_{\mu4}^{tr}$ are defined in Eqs. (6) and (7), E is an incident muon neutrino energy, $v = \sqrt{E^2 - m_s^2}/E$ and θ is an angle between muon neutrino 3-momentum and sterile neutrino 3-momentum in the laboratory frame. Equation (10) generalizes Eq. (4) of Ref. [10] to the case of models where electric and magnetic transition moments are presented.

For muon antineutrino the conversion cross section is:

$$\frac{d\sigma_{\mp}^{\bar{\nu}}(E,\theta,\phi)}{d\cos\theta d\phi} = \frac{\alpha\left(\kappa_{\mu4}^{tr}\right)^2}{4\pi}\left(1 + \sin\left(2\lambda_{\mu4}^{tr}\right)\cos\left(\phi_{\mu4}^{tr} - \chi_{\mu4}^{tr}\right)\right)\frac{G^2(t)}{t^2}vE^4(1\pm v)^3(1\mp\cos\theta) \ . \quad (11)$$

We see that neutrino and antineutrino cross sections complement each other in the following sense: at least one of them is non-zero for any choice of phases $\lambda_{\mu4}^{tr}$, $\phi_{\mu4}^{tr}$, $\chi_{\mu4}^{tr}$ if $\kappa_{\mu4}^{tr}$ is non-zero. Combined with analogous property of sterile neutrino decay rate (see Eqs. (12) and (13)), it would follow that we can limit the value of $\kappa_{\mu4}^{tr}$. Note in passing that in Eqs. (10) and (11) we assume that quasi-elastic processes dominate and the energy of heavy neutrino is equal to the incident muon neutrino energy.

Let us proceed with a description of heavy sterile (anti)neutrino radiative decay. The (anti)neutrino decays into some other (anti)neutrino of significantly smaller[2] mass ($m_j \ll m_s$) and photon. Formulas for differential decay rates of sterile (anti)neutrino of a given chirality (±) are:

$$\frac{d\Gamma_{\pm}^{\nu}}{d\phi_\gamma d\cos\theta_\gamma} = \frac{1}{32\pi^2}m_s^3\sum_{i=1}^{3}\left(\kappa_{4i}^{tr}\right)^2\left(1 \mp \sin\left(2\lambda_{4i}^{tr}\right)\cos\left(\phi_{4i}^{tr} - \chi_{4i}^{tr}\right)\cos\left(\theta_\gamma\right)\right) \ , \quad (12)$$

$$\frac{d\Gamma_{\pm}^{\overline{\nu}}}{d\phi_\gamma d\cos\theta_\gamma} = \frac{1}{32\pi^2}m_s^3\sum_{i=1}^{3}\left(\kappa_{4i}^{tr}\right)^2\left(1 \pm \sin\left(2\lambda_{4i}^{tr}\right)\cos\left(\phi_{4i}^{tr} - \chi_{4i}^{tr}\right)\cos\left(\theta_\gamma\right)\right) \ , \quad (13)$$

where θ_γ and ϕ_γ are polar and azimuthal angles of out-coming photon's 3-momentum in the sterile neutrino rest frame measured from the 3-momentum of heavy neutrino in the laboratory frame. As we see, generally there is an anisotropy in polar angle in Eqs. (12) and (13).

The full width is (see e.g. [13]):

$$\Gamma = \Gamma_{\pm}^{\nu} = \Gamma_{\pm}^{\overline{\nu}} = \frac{1}{8\pi}m_s^3\sum_{i=1}^{3}\left(\kappa_{4i}^{tr}\right)^2 \ . \quad (14)$$

The difference between the Majorana and the Dirac neutrinos just slightly modifies formulas and to get constraints for the Majorana case one should substitute everywhere $\kappa_{\mu4}$ by $2\kappa_{\mu4}$ and κ_{4i} by $2\kappa_{4i}$. In this paper we present constraints for the Dirac neutrinos. In the case of the Majorana neutrinos one should divide the obtained constraints on $\kappa_{\mu4}$ for the Dirac case by a factor two.

---

[2] It is important that final (anti)neutrinos have significantly smaller mass in comparison with m_s, otherwise the spectra get shifted towards small energies and all further calculations have to be modified, as we do in Section 4.

3 Theoretical predictions

In this Section we derive approximate analytical formulas for the number of photon events associated with sterile neutrinos could be observed in the MiniBooNE detector. The MiniBooNE experiment has two operating modes ($\boldsymbol{mode} \in \{\boldsymbol{neutrino}, \boldsymbol{antineutrino}\}$). In the neutrino mode there is a dominant flux of muon neutrinos and a subdominant flux of muon antineutrinos, in the antineutrino mode there is a dominant flux of muon antineutrinos and a subdominant flux of muon neutrinos [14] (electron neutrinos don't play any role in our analysis and they are neglected in what follows). It should be emphasized that these two fluxes would be independent sources of photons.

Everywhere we use following notations for angle coordinates: (θ,ϕ) are for converted heavy neutrinos in the laboratory frame, (θ_γ,ϕ_γ) are for photons in the heavy neutrino rest frame, (θ_{det},ϕ_{det}) are for photons in the laboratory frame.

Bins for distributions of events of reconstructed quasi-elastic energy (evaluated from visible energy and polar angle, see Eq. (3) of Ref. [15]) are: [1, 2, 3]:

$$\boldsymbol{bin} = [\boldsymbol{E^{QE}_{min}}, \boldsymbol{E^{QE}_{max}}] \in \{\mathbf{[0.2\ GeV, 0.3\ GeV],\ [0.3\ GeV, 0.375\ GeV],\ etc.}\}\ , \tag{15}$$

visible energy bins [2, 3]:

$$\boldsymbol{bin} = [\boldsymbol{E_{min}}, \boldsymbol{E_{max}}] \in \{\mathbf{[0.1\ GeV, 0.2\ GeV],\ [0.2\ GeV, 0.3\ GeV],\ etc.}\}\ , \tag{16}$$

and polar angle bins [1, 2]:

$$\boldsymbol{bin} = [\mathbf{cos}\,\boldsymbol{\theta_{min}}, \mathbf{cos}\,\boldsymbol{\theta_{max}}] \in \{\mathbf{[-1.0, -0.8],\ [-0.8, -0.6],\ etc.}\}\ . \tag{17}$$

In each bin we compare the number of events expected due to dipole interactions with the number of *the anomalous events* (the excess is defined as difference between numbers of events observed and events predicted by the Standard model with three active massive neutrinos). For the energy range of detected photons under investigation the predictions depend monotonically on the energy of detected photons. The difference between visible and reconstructed quasi-elastic energies of photon is negative and negligible for photons with small polar angles θ_{det} in comparison with detector resolution and bin sizes. So it is reasonable to neglect the difference between visible and reconstructed energies since almost all predicted events have very small polar angle θ_{det} (see Fig. 3).

The efficiency of the MiniBooNE detector $\epsilon_\gamma(E)$ to register photon is determined as a piecewise function of visible energy [3]. So for energy distributions we set the efficiency inside each bin as corresponding constant. For polar angle distribution to simplify calculations we set efficiency to its minimal value $\epsilon_\gamma = 7.3\%$, when we work on constraints (this gives a conservative constraints for photon energies below $E_\gamma < 1.5$ GeV). It is justified by a very moderate dependence of results (limits on $\kappa^{tr}_{\mu 4}$) on the efficiency variation.

To be observed sterile neutrinos has to decay inside a sphere of radius $R = 5.0\,\text{m}$. The MiniBooNE detector is located far away from the beam target, so heavy (anti)neutrino fluxes are approximately homogeneous over the volume of spherical detector. For sterile neutrino of the energy E we define the average probability of the decay inside the inner sphere. Because heavy neutrinos could be produced everywhere inside the inner sphere, it is evaluated by averaging the probability for heavy neutrino to decay inside it:

$$P(x) = \frac{1}{4/3\pi R^3}\int_0^R 2\pi r dr \int_0^{2\sqrt{R^2-r^2}} \left(1 - \exp\left(\frac{-xz}{R}\right)\right) dz\ , \tag{18}$$

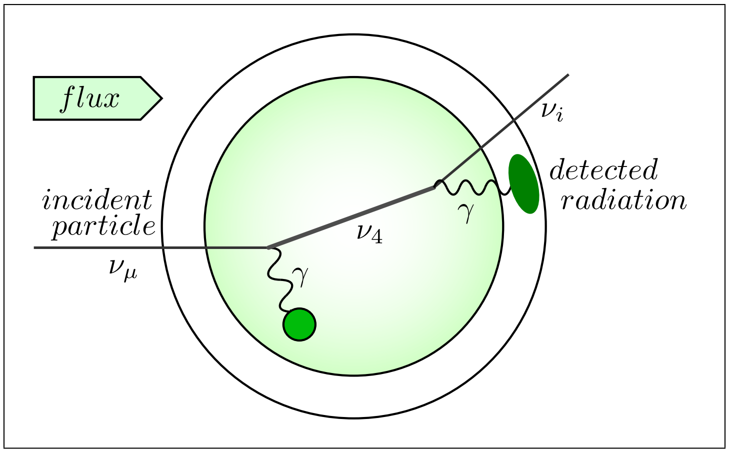

Figure 1: Schematic illustration of the conversion and decay of the ν_4 in the MiniBooNE detector.

where a dimensionless parameter x is defined as a product of inverse decay length and the radius of the inner sphere:

$$x = \frac{m_s^3 \kappa^2}{8\pi} \frac{m_s}{\sqrt{E^2 - m_s^2}} R \, . \tag{19}$$

Integral (18) is equal to:

$$P\left(x\right) = 1 - \frac{3\left(2x^2 - 1 + \left(2x + 1\right) e^{-2x}\right)}{8x^3} \, . \tag{20}$$

Below, we obtain theoretical predictions for distributions of visible energy and polar angle and discuss approximations we use in calculations of constraints.

From Eqs. (20), (10) and (12), (11) and (13) we give an analytical estimate for the number of events in both operating modes of the MiniBooNE experiment. We introduce two functions: the first corresponds to isotropic part of differential decay rates (12) and (13) (θ_γ-independent terms):

$$\begin{split}\mathcal{A}^{mode,particle}_{[E_{min},E_{max}]} = \left(\kappa^{tr}_{\mu 4}\right)^2 \frac{\alpha}{4} \mathcal{N}^{mode}_{p.o.t.} N_C \epsilon_\gamma \int dE \, d\cos\theta E^3 \sqrt{E^2 - m_s^2} \rho^{particle}_{mode}(E) \frac{G^2\left(t\right)}{t^2} P\left(x\right) \times \\ \times \left(\left(1+v\right)^3\left(1 - \cos\theta\right) + \left(1-v\right)^3\left(1 + \cos\theta\right)\right)\left(\cos\theta_{cut}(E_{max}) - \cos\theta_{cut}(E_{min})\right) \; ;\end{split} \tag{21}$$

the second corresponds to anisotropic part of differential decay rates (12) and (13) (θ_γ-dependent term):

$$\begin{split}\mathcal{B}^{mode,particle}_{[E_{min},E_{max}]} = \left(\kappa^{tr}_{\mu 4}\right)^2 \frac{\alpha}{8} \mathcal{N}^{mode}_{p.o.t.} N_C \epsilon_\gamma \int dE \, d\cos\theta E^3 \sqrt{E^2 - m_s^2} \rho^{particle}_{mode}(E) \frac{G^2\left(t\right)}{t^2} P\left(x\right) \times \\ \times \left(\left(1+v\right)^3\left(1 - \cos\theta\right) - \left(1-v\right)^3\left(1 + \cos\theta\right)\right)\left(\cos^2\theta_{cut}(E_{max}) - \cos^2\theta_{cut}(E_{min})\right) \; ,\end{split} \tag{22}$$

where $\rho^{(anti)neutrino}_{mode}(E)$ is a muon (anti)neutrino energy spectrum in a given operating mode [14], $\epsilon_\gamma = \epsilon_\gamma(0.5\left(E_{min} + E_{max}\right))$ is the detection efficiency, $\mathcal{N}^{mode}_{p.o.t.}$ is a number of protons on target, $N_C = \left(5.0/6.1\right)^3 \times 3.5 \times 10^{31}$ is a number of carbon atoms inside the inner sphere and a function

$\cos\theta_{cut}(E)$ is defined as:

$$\cos\theta_{cut}(E) = \begin{cases} -1, & \text{at} \quad E < \frac{m_s}{2}\sqrt{\frac{1-v}{1+v}} \\ \frac{1}{v}\left(\frac{2E}{m_s}\sqrt{1-v^2}-1\right), & \text{at} \quad \frac{m_s}{2}\sqrt{\frac{1-v}{1+v}} \le E \le \frac{m_s}{2}\sqrt{\frac{1+v}{1-v}} \\ 1, & \text{at} \quad E > \frac{m_s}{2}\sqrt{\frac{1+v}{1-v}}\ . \end{cases} \tag{23}$$

In a given bin the predicted number of events is defined as:

$$\begin{aligned} \mathcal{N}^{mode}_{[E_{min},E_{max}]} = (1-\sin(2\lambda_\mu))\left(\mathcal{A}^{mode,neutrino}_{[E_{min},E_{max}]} - \sin(2\lambda_4)\mathcal{B}^{mode,neutrino}_{[E_{min},E_{max}]}\right) + \\ + (1+\sin(2\lambda_\mu))\left(\mathcal{A}^{mode,antineutrino}_{[E_{min},E_{max}]} + \sin(2\lambda_4)\mathcal{B}^{mode,antineutrino}_{[E_{min},E_{max}]}\right)\ , \end{aligned} \tag{24}$$

where we introduced variables:

$$\sin(2\lambda_\mu) \equiv \sin\left(2\lambda^{tr}_{\mu 4}\right)\cos\left(\phi^{tr}_{\mu 4} - \chi^{tr}_{\mu 4}\right) \quad \text{and} \quad \sin(2\lambda_4) \equiv \sum_{i=1}^{3} \frac{\left(\kappa^{tr}_{4i}\right)^2}{\kappa^2} \sin(2\lambda_{4i})\cos\left(\phi^{tr}_{4i} - \chi^{tr}_{4i}\right)\ . \tag{25}$$

Note that if $\cos\theta_{cut}(E_{min}) < \cos\theta_{cut}(E_{max})$ then:

$$|\mathcal{B}^{mode,particle}_{[E_{min},E_{max}]}| < \mathcal{A}^{mode,particle}_{[E_{min},E_{max}]}\ , \tag{26}$$

and, consequently, the predicted number of events (see Eq. (24)) would be non-zero for all values of parameters λ_μ and λ_4.

It is important that theoretically predicted number of events (24) depends *monotonically* on parameters $\kappa^{tr}_{\mu 4}$ and κ^{tr}_{i4}. Provided the approximate relation:

$$\sum_{i=1}^{3}\left(\kappa^{tr}_{4i}\right)^2 \ge \left(\kappa^{tr}_{\mu 4}\right)^2\ , \tag{27}$$

which is valid up to neglected flavor mixing between active and sterile neutrinos, we place constraints from above on possible values of $\kappa^{tr}_{\mu 4}$. Indeed, if we substitute everywhere the combination $\sum_{i=1}^{3}\left(\kappa^{tr}_{4i}\right)^2$ by $\left(\kappa^{tr}_{\mu 4}\right)^2$, it would only suppress the predicted number of events (24). Otherwise, if the relation (27) is invalid and hence flavor mixing between sterile and active neutrino is significant, constraints will depend not only on the mass of sterile neutrino but on its lifetime as well.

In Fig. 2 we compare the predicted number of events $\mathcal{N}^{mode}_{[E_{min},E_{max}]}$ at parameter values $m_s = 50$ MeV, $\kappa^{tr}_{\mu 4} = 9.9\times 10^{-9}\mu_B$, $\tau = 1/\Gamma = 1.5\times 10^{-8}\ s$, $\sin(2\lambda_4) = 0$, $\sin(2\lambda_\mu) = 0$ to observed energy distributions of excess events obtained in both operating modes.

Then we investigate event distribution of polar angle. We introduce polar angle θ_{det} and azimuthal angle ϕ_{det} between the muon neutrino beam axis and detected photon's 3-momentum. It is related to previously introduced polar angle θ_γ for a given polar angle θ:

$$\cos\theta_\gamma = \frac{\cos\theta_{det}\cos\theta + \sin\theta_{det}\sin\theta\cos\phi_{det} - v}{1 - v\left(\cos\theta_{det}\cos\theta + \sin\theta_{det}\sin\theta\cos\phi_{det}\right)}\ , \tag{28}$$

To define the predicted number of events we need to cast Eqs. (12) and (13) in terms of new angles $(\theta_{det}, \phi_{det})$. The integration measure is transformed as:

$$d\cos\theta_\gamma d\phi_\gamma = \frac{(1-v^2)\, d\cos\theta_{det} d\phi_{det}}{\left(1 - v\left(\cos\theta_{det}\cos\theta + \sin\theta_{det}\sin\theta\cos\phi_{det}\right)\right)^2}\ . \tag{29}$$

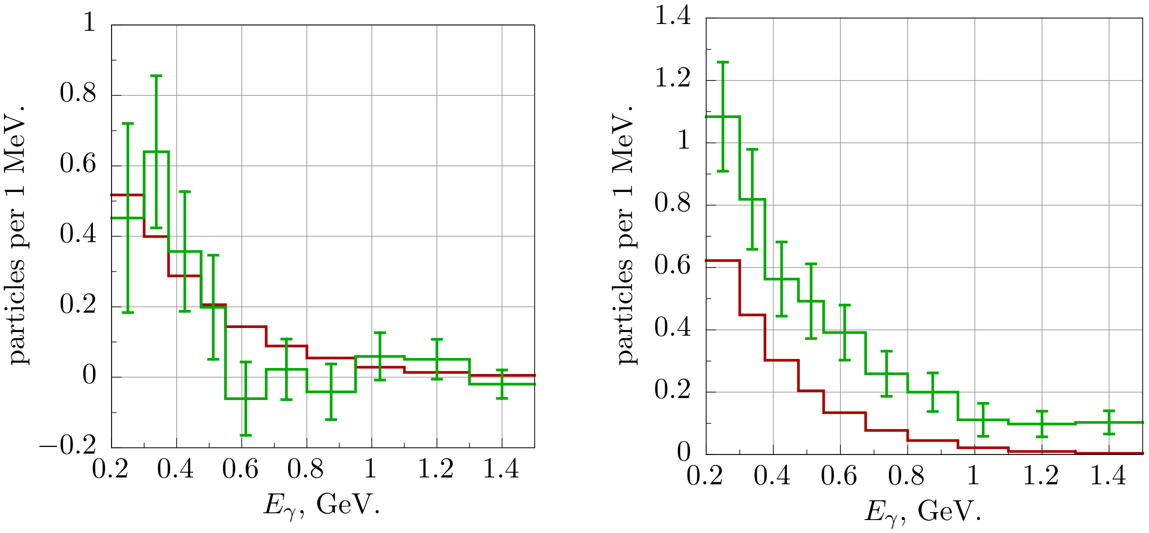

Figure 2: Energy distributions of excess events obtained in neutrino (left) and antineutrino (right) with error bars [3] and corresponding predicted spectra of photons $\mathcal{N}^{mode}_{[E_{min},E_{max}]}$ from sterile neutrino decays at parameter values $m_s = 50$ MeV, $\kappa^{tr}_{\mu 4} = 9.9 \times 10^{-9}\mu_B$, $\tau = 1/\Gamma = 1.5 \times 10^{-8}$ s, $\sin(2\lambda_4) = 0$, $\sin(2\lambda_\mu) = 0$.

Using Eqs. (28) and (29) we transform decay rates (12) and (13) into new variables θ_{det} and ϕ_{det}. Analogously to the previous case we introduce two functions:

$$\begin{aligned}\mathcal{U}^{mode,particle}_{[\cos\theta_{min},\cos\theta_{max}]} &= \left(\kappa^{tr}_{\mu 4}\right)^2 \frac{\alpha}{8\pi}\mathcal{N}^{mode}_{p.o.t.} N_C \int \frac{\left(1-v^2\right) dE\, d\cos\theta\, d\cos\theta_{det} d\phi_{\rm det}}{\left(1 - v\left(\cos\theta_{det}\cos\theta + \sin\theta_{det}\sin\theta\cos\phi_{det}\right)\right)^2} \times \\ &\times E^3\sqrt{E^2 - m_s^2}\,\epsilon_\gamma \rho^{particle}_{mode}(E)\,\frac{G^2(t)}{t^2}\left(\left(1+v\right)^3\left(1-\cos\theta\right) + \left(1-v\right)^3\left(1+\cos\theta\right)\right) P(x) \times \\ &\times\Theta\left(1 + v\left(\cos\theta_{det}\cos\theta + \sin\theta_{det}\sin\theta\cos\phi_{det}\right) - \frac{2\sqrt{1-v^2}E_{min}}{m_s}\right) ,\end{aligned} \tag{30}$$

$$\begin{aligned}\mathcal{V}^{mode,particle}_{[\cos\theta_{min},\cos\theta_{max}]} &= \left(\kappa^{tr}_{\mu 4}\right)^2 \frac{\alpha}{8\pi}\mathcal{N}^{mode}_{p.o.t.} N_C \int \frac{\left(1-v^2\right) dE\, d\cos\theta\, d\cos\theta_{det} d\phi_{\rm det}}{\left(1 - v\left(\cos\theta_{det}\cos\theta + \sin\theta_{det}\sin\theta\cos\phi_{det}\right)\right)^3} \times \\ &\times\left(\cos\theta_{det}\cos\theta + \sin\theta_{det}\sin\theta\cos\phi_{det} - v\right) E^3\sqrt{E^2 - m_s^2}\,\epsilon_\gamma \rho^{particle}_{mode}(E)\,\frac{G^2(t)}{t^2} \times \\ &\times\left(\left(1+v\right)^3\left(1-\cos\theta\right) - \left(1-v\right)^3\left(1+\cos\theta\right)\right) P(x) \times \\ &\times\Theta\left(1 + v\left(\cos\theta_{det}\cos\theta + \sin\theta_{det}\sin\theta\cos\phi_{det}\right) - \frac{2\sqrt{1-v^2}E_{min}}{m_s}\right) ,\end{aligned} \tag{31}$$

where we integrate over ϕ from 0 to 2π and over $\cos\theta_{det}$ from $\cos\theta_{max}$ to $\cos\theta_{min}$, Θ is the step function, which selects events with visible photon energies $E_\gamma > E_{min} = 0.2$ GeV. Then theoretical prediction for a number of events by $\cos\theta_{det}$ with visible photon energies $E_\gamma > E_{min}$ is:

$$\begin{aligned}\mathcal{N}^{mode}_{[\cos\theta_{min},\cos\theta_{max}]} &= \left(1 - \sin\left(2\lambda_\mu\right)\right)\left(\mathcal{U}^{mode,particle}_{[\cos\theta_{min},\cos\theta_{max}]} - \sin\left(2\lambda_4\right)\mathcal{V}^{mode,particle}_{[\cos\theta_{min},\cos\theta_{max}]}\right) + \\ &+ \left(1 + \sin\left(2\lambda_\mu\right)\right)\left(\mathcal{U}^{mode,particle}_{[\cos\theta_{min},\cos\theta_{max}]} + \sin\left(2\lambda_4\right)\mathcal{V}^{mode,particle}_{[\cos\theta_{min},\cos\theta_{max}]}\right) .\end{aligned} \tag{32}$$

Figure 3 demonstrates that almost all photons would be produced in the forward direction. To properly constrain $\kappa_{\mu 4}$ from polar angle distributions one needs to know the uncertainties for the excess events. However, we did not find these estimates in literature, and thus do not use polar angle distribution to place limit on $\kappa_{\mu 4}$. Note in passing that the excess distribution of $\cos\theta_{det}$ remains intact with decrease of sterile neutrino lifetime (e.g. if other decay modes are introduced). Indeed, the decrease of lifetime would just add more energetic photons and increase the peak in the forward direction, because the function (20) suppresses high energetic particles stronger than low energetic ones and has a limit equal to one at big arguments.

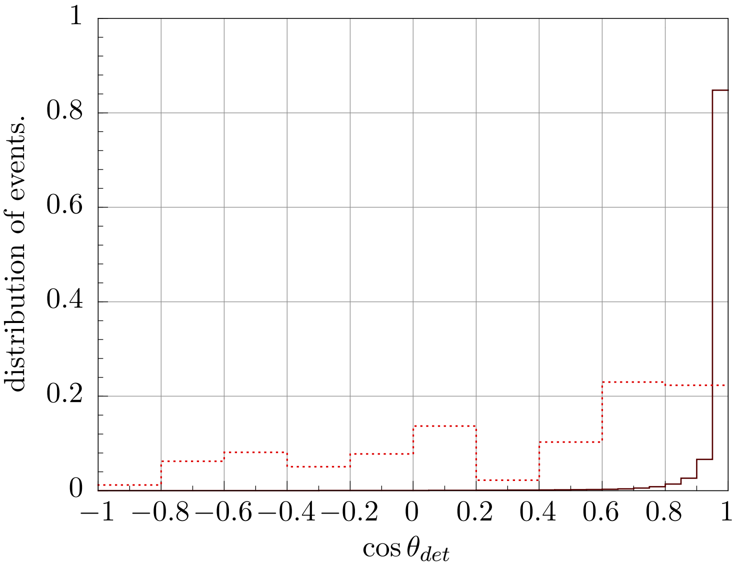

Figure 3: Theoretically predicted events as a function of $\cos\theta_{det}$ in the neutrino operating mode at $m_s = 50$ MeV, $\kappa^{tr}_{\mu 4} = 1 \times 10^{-9}\mu_B$, $\tau = 1/\Gamma = 1.5 \times 10^{-6}$, $\sin(2\lambda_\mu) = 0$, $\sin(2\lambda_4) = 0$ (solid line) and the observed excess (the dashed line) [3].

4 Analysis methods and results

As follows from fitting theoretically predicted numbers of events (32) to the excess distributions, the anomalies [1, 2, 3] cannot be entirely explained only by the effective dipole electromagnetic interaction (5). For this reason we: (*i*) work on constraints, but not on the expected values of parameters, which will explain anomalies; (*ii*) analyze each bin and each mode independently.

We find numbers of events as functions of $\kappa^{tr}_{\mu 4}$, $\sin\lambda_\mu$ and $\sin\lambda_4$ for all bins and modes from (24). After these calculations, using known uncertainties of the experimental results for each bin and mode, we investigate the predicted numbers of events as functions of $\sin\lambda_\mu$, $\sin\lambda_4$ and m_s. In each bin we constrain $\kappa^{tr}_{\mu 4}(\sin\lambda_\mu, \sin\lambda_4, m_s)$ at 95% C.L.. Then we finally constrain $\kappa^{tr}_{\mu 4}$ for a given m_s by the minimum value over all bins and modes and the maximum value over continuous variables $\sin\lambda_\mu$ and $\sin\lambda_4$ of the constraints on $\kappa^{tr}_{\mu 4}(\sin\lambda_\mu, \sin\lambda_4, m_s)$.

In Fig. 4 (left) the upper limit on $\kappa^{tr}_{\mu 4}$ at 95% C.L. is shown and in Fig. 4 (right) we present constraint on sterile neutrino mean life time, derived from the upper limit on $\kappa^{tr}_{\mu 4}$ (provided Eq. (27)).

We see that data from the MiniBooNE detector allow to improve constraints [10] for the mass range $m_s < 350$ MeV.

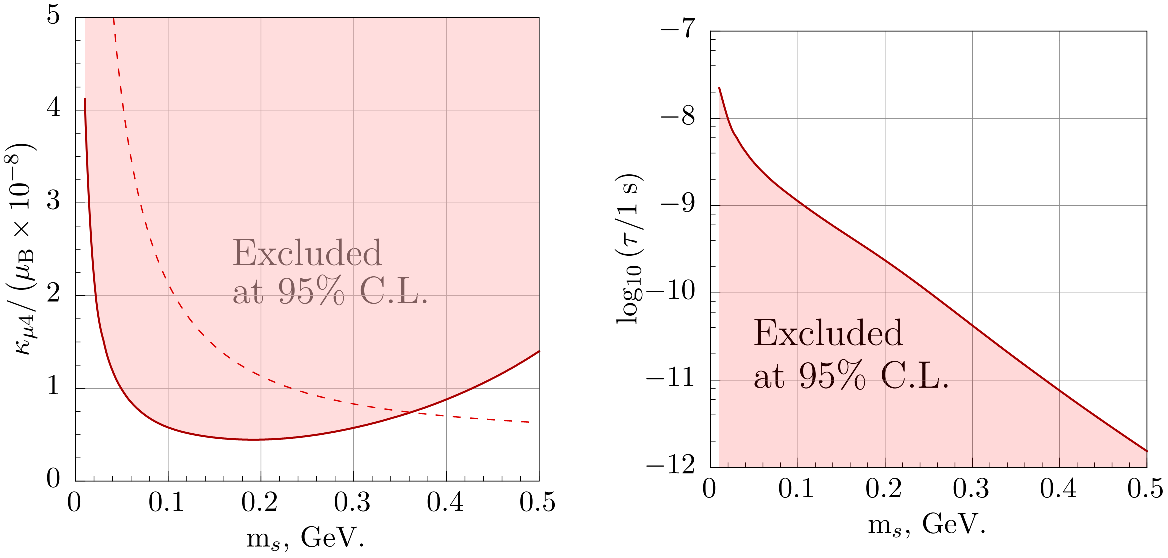

Figure 4: In the left plot the shaded area in $\left(m_s,\ \kappa^{tr}_{\mu 4}\right)$ is excluded at 95% C.L. from our analysis. The region above the dashed line was excluded in Ref. [10]. In the right plot we present constraints on sterile neutrino lifetime obtained from constraints on $\kappa^{tr}_{\mu 4}$.

Now let us discuss a modification of the previous analysis to the models with more sterile neutrinos ($N_\nu \geq 5$). In particular ν_s may decay into γ and new sterile neutrino(s) $\nu_{s,j}$ ($j \geq 5$), if kinematically allowed, i.e. $m_s > m_{s,j}$. Eqs. (12) and (13) take different forms:

$$\begin{aligned}\frac{d\Gamma^{\nu}_{\pm}}{d\phi_\gamma d\cos\theta_\gamma} &= \frac{1}{32\pi^2} m_s^3 \sum_{i=1}^{3} \left(\kappa^{tr}_{4i}\right)^2 \left(1 \mp \sin\left(2\lambda^{tr}_{4i}\right)\cos\left(\phi^{tr}_{4i} - \chi^{tr}_{4s,j}\right)\cos\left(\theta_\gamma\right)\right) + \\ &+ \frac{1}{32\pi^2} m_s^3 \sum_{j=5}^{N_\nu} \Theta\left(m_s - m_{s,j}\right)\left(1 - \frac{m_{s,j}^2}{m_s^2}\right)^3 \left(\kappa^{tr}_{4s,j}\right)^2 \times \\ &\times \left(1 \mp \sin\left(2\lambda^{tr}_{4s,j}\right)\cos\left(\phi^{tr}_{4s,j} - \chi^{tr}_{4s,j}\right)\cos\left(\theta_\gamma\right)\right)\ ,\end{aligned} \tag{33}$$

$$\begin{aligned}\frac{d\Gamma^{\overline{\nu}}_{\pm}}{d\phi_\gamma d\cos\theta_\gamma} &= \frac{1}{32\pi^2} m_s^3 \sum_{i=1}^{3} \left(\kappa^{tr}_{4i}\right)^2 \left(1 \pm \sin\left(2\lambda^{tr}_{4i}\right)\cos\left(\phi^{tr}_{4i} - \chi^{tr}_{4s,j}\right)\cos\left(\theta_\gamma\right)\right) + \\ &+ \frac{1}{32\pi^2} m_s^3 \sum_{j=5}^{N_\nu} \Theta(m_s - m_{s,j})\left(1 - \frac{m_{s,j}^2}{m_s^2}\right)^3 \left(\kappa^{tr}_{4s,j}\right)^2 \times \\ &\times \left(1 \pm \sin\left(2\lambda^{tr}_{4s,j}\right)\cos\left(\phi^{tr}_{4s,j} - \chi^{tr}_{4s,j}\right)\cos\left(\theta_\gamma\right)\right)\ .\end{aligned} \tag{34}$$

The energy of the outgoing photon as the function of E and $\cos\theta$ is determined through:

$$E_\gamma = \frac{m_s}{2}\left(1 - \frac{m_{s,j}^2}{m_s^2}\right)\frac{1 + v\cos\theta}{\sqrt{1 - v^2}}\ . \tag{35}$$

And consequently we have to introduce modifications of the cutoff function θ_{cut} (see Eq. (23)), which now depends on $m_{s,j}$:

$$\cos\theta^{s,j}_{cut}(E) = \cos\theta_{cut}\left(\frac{E}{\left(1-\frac{m^2_{s,j}}{m^2_s}\right)}\right) . \tag{36}$$

We are ready now to discuss the second mentioned in Introduction scenario [9] suggested to explain MiniBooNE and LSND anomalies. Initially it contained flavor mixing between sterile and muon neutrinos, but such mixing was found inconsistent with kaon decays [6]. Then the authors of [9] have introduced two sterile Majorana neutrinos: $m_s = 50$ MeV, 5 MeV $< m_{s,5} <$ 10 MeV and two transition magnetic dipole moments $\mu^{tr}_{\mu 4} = 2.4 \times 10^{-9}\mu_B$ and $\mu^{tr}_{45} = 2.4 \times 10^{-8}\mu_B$, the latter saturates the heavy sterile neutrino decay rate via $\nu_s \to \nu_{s,j}\gamma$. Equation (35) implies that massless approximation is reasonable for such hierarchy of m_s and $m_{s,5}$. To test the case with two sterile neutrinos we fix the proposed relation between magnetic moments $\mu^{tr}_{\mu 4} = 0.1 \times \mu^{tr}_{45}$. And using Eq. (24) we place constraint $\mu^{tr}_{45} < 2.1 \times 10^{-8}\mu_B$ (95% C.L.) for the Majorana neutrinos, which is marginally consistent with the given value μ^{tr}_{45}. However, evidently such model is disfavored, because additional source of photons would give a peak in the forward direction. Extensions of the obtained constrains to the models with several neutrinos are straightforward. More careful analysis is required to test models with almost degenerate (in masses) sterile neutrinos. In particular, in the model with two degenerate neutrinos $m_4 \approx m_{s,5}$ for $\left(\kappa^{tr}_{45}\right)^2\left(1 - m^2_{s,5}/m^2_s\right)^3 \gg \left(\kappa^{tr}_{\mu 4}\right)^2$ most photons from decays $\nu_4 \to \nu_{s,5}\gamma$ could have energies comparable or below lower energy cut off at 200 MeV. In such specific case sterile neutrino could avoid ours constraints for κ^{tr}_{45} and $\kappa^{tr}_{\mu 4}$. But such situation is excluded as the explanation of the excess, because experimental data shows smooth angular dependence [3].

5 Conclusion

Combined analysis from different focusing regimes of the MiniBooNE detector have allowed us to investigate models with heavy sterile neutrinos. Particularly we renewed and generalized constraints on electromagnetic transition dipole moments. The main results are presented in Fig. 4. The obtained analytical formulas are rather general and applicable for other neutrinos experiments.

We have shown that sterile neutrino of mass 10 MeV $< m_s <$ 500 MeV with transition dipole moments and without significant mixing with active neutrinos of the mass in the region 10 MeV $< m_s <$ 500 MeV, cannot explain anomalies if one regards MiniBooNE polar angle distribution of the anomalous events.

Acknowledgements

We thank D. S. Gorbunov and S. N. Gninenko for stimulating questions and fruitful discussions. The work is partially supported by the grant of the Ministry of Education and Science No. 8412, the grant of the President of the Russian Federation NS-5590.2012.2 and the RFBR grant 13-02-01127.

References

[1] A. Aguilar-Arevalo et al. (MiniBooNE Collaboration), Phys.Rev.Lett. **102**, 101802 (2009), `0812.2243`.

[2] A. Aguilar-Arevalo et al. (MiniBooNE Collaboration), Phys.Rev.Lett. **105**, 181801 (2010), `1007.1150`.

[3] A. Aguilar-Arevalo et al. (MiniBooNE Collaboration) (2012), `1207.4809`.

[4] S. N. Gninenko, Phys.Rev. **D83**, 015015 (2011), `1009.5536`.

[5] S. Gninenko, Phys.Lett. **B710**, 86 (2012), `1201.5194`.

[6] V. Duk et al. (ISTRA+ Collaboration), Phys.Lett. **B710**, 307 (2012), `1110.1610`.

[7] S. Gninenko, Phys.Rev.Lett. **103**, 241802 (2009), `0902.3802`.

[8] S. Gninenko and D. Gorbunov, Phys.Rev. **D81**, 075013 (2010), `0907.4666`.

[9] M. Masip, P. Masjuan, and D. Meloni (2012), `1210.1519`.

[10] S. Gninenko and N. Krasnikov, Phys.Lett. **B450**, 165 (1999), `hep-ph/9808370`.

[11] A. Aguilar-Arevalo et al. (MiniBooNE Collaboration), Nucl.Instrum.Meth. **A599**, 28 (2009), `0806.4201`.

[12] Y.-S. Tsai, Rev.Mod.Phys. **46**, 815 (1974).

[13] R. N. Mohapatra and P. B. Pal, *Massive Neutrinos in Physics and Astrophysics; 3rd ed.*, World Scientific Lecture Notes in Physics (World Scientific, Singapore, 2004).

[14] A. Aguilar-Arevalo et al. (MiniBooNE Collaboration), Phys.Rev. **D79**, 072002 (2009), `0806.1449`.

[15] A. Aguilar-Arevalo et al. (MiniBooNE Collaboration), Phys.Rev.Lett. **100**, 032301 (2008), `0706.0926`.